Journal of Oceanography (2018) 74:499–508
https://doi.org/10.1007/s10872-018-0475-z

ORIGINAL ARTICLE

Coastal upwelling events along the southern coast of Java during the 2008 positive Indian Ocean Dipole

T. Horii[1] · I. Ueki[1] · K. Ando[1]

Received: 19 November 2017 / Revised: 10 April 2018 / Accepted: 12 April 2018 / Published online: 20 April 2018

Abstract
To understand the coastal upwelling system along the southern coast of Java, we investigated ocean temperature and salinity obtained from an Argo float. In 2008, a positive Indian Ocean Dipole (IOD) event began to develop in early May and anomalously cool SST developed around south of Java from May to September. During the peak of the IOD, an Argo float successfully observed vertical structure of temperature and salinity within 90 km from Java. The float observed two intraseasonal-scale temperature cooling events in July and August, with significant upward movements of the thermocline more than 90 m. Concurrent with the signals, anomalous southeasterly alongshore winds, lowering of local SST and sea level, and upward expansion of high-salinity water were also observed. During the event in August, vertical velocity estimated by the anomalous wind stress agreed well with the observations. These results indicate that the Argo float observed the coastal upwelling, which was enhanced by the 2008 positive IOD, along the southern coast of Java.

Keywords Coastal upwelling · South of Java · Argo float · Sea level · Indian Ocean Dipole · Indian Ocean warm pool · Air-sea interaction

1 Introduction

The high sea surface temperature (SST) and the surrounding SST gradient over the eastern Indian Ocean warm pool induce active air-sea interaction (see Schott et al. 2009 for a review). Sumatra and Java in Indonesia are located in the southeastern edge of the warm pool, and form part of the eastern boundary of the tropical Indian Ocean (Fig. 1a, b). Previous studies have reported that there are coastal upwelling signals along the southwestern coasts of Sumatra and Java due to southeasterly wind during the boreal summer monsoon (e.g. Wyrtki 1962; Bray et al. 1996). In June to September, a southeasterly monsoonal wind prevails along the coasts and surrounding offshore areas. Resultant Ekman transport and coastal upwelling replace surface warm water with cool and nutrient-rich water from underneath (Susanto et al. 2001; Susanto and Marra 2005; Iskandar et al. 2009). The coastal upwelling plays an important role in the ocean surface heat balance (Du et al. 2005; Chen et al. 2016), biogeochemical balance, coastal ecosystem and fisheries (Farley and Davis 1998) in the area. The average SST off the southern coast of Java is more than 1 °C lower than the surroundings, suggesting that the coastal upwelling can potentially have an impact on the formation of regional climate conditions.

The strength of the coastal upwelling is closely linked to the El Niño/Southern Oscillation (ENSO; e.g. Susanto et al. 2001; Susanto and Marra 2005; Ningsih et al. 2013) and the Indian Ocean Dipole (IOD; e.g. Saji et al. 1999; Webster et al. 1999; Delman et al. 2016). In the developing phase of a positive IOD, the upwelling of subsurface cold water along the coasts of Sumatra and Java expands westward and produces a large zonal SST gradient in the central-eastern tropical Indian Ocean. The resultant atmospheric pressure gradient intensifies southeasterly wind anomalies along the coasts. The wind anomalies further strengthen the SST gradient through enhancement of the upwelling. This ocean–atmosphere feedback process associated with ocean upwelling was originally indicated by Saji et al. (1999) and Webster et al. (1999), and has been reproduced by numerical models (e.g. Murtugudde et al. 2000; Iizuka et al. 2000;

✉ T. Horii
horiit@jamstec.go.jp

[1] Research and Development Center for Global Change (RCGC), Japan Agency for Marine-Earth Science and Technology (JAMSTEC), 2-15, Natsushima, Yokosuka, Kanagawa 237-0061, Japan

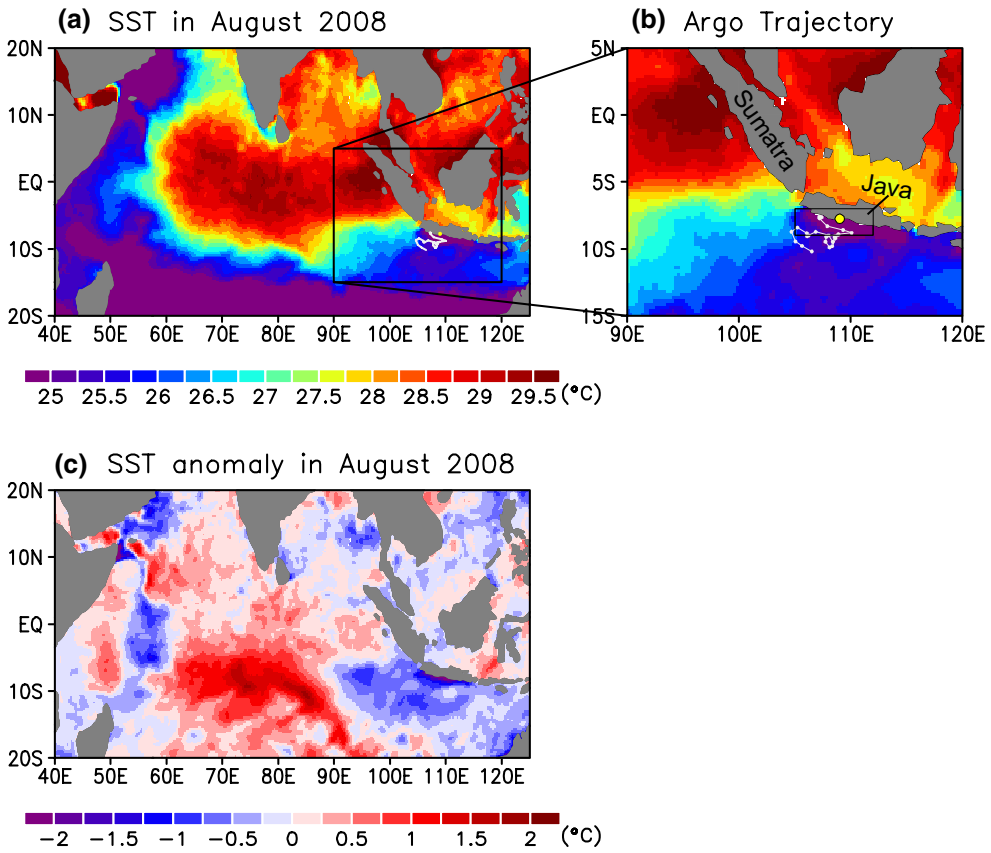

Fig. 1 **a** SST in August 2008. **b** As in Fig. 1a, but for the southwestern region of Sumatra and Java. White lines (circles) indicate trajectories (observation points) of an Argo float during 2008. A yellow circle at 7.8°S, 109°E indicates the location of an Indonesian tidal station (Cilacap). The black box shows the average area of SST and winds shown in Fig. 2a. **c** As in **a**, but for SST anomalies

Vinayachandran et al. 2002; Halkides and Lee 2009; Chen et al. 2015), and also identified by in situ observations (Horii et al. 2009). The year-to-year variability and upwelling processes have also been investigated (Chen et al. 2016; Delman et al. 2016). Using a high-resolution ocean model, Chen et al. (2016) indicated that interannual variability of the coastal upwelling was mainly controlled by remote forcing from equatorial Indian Ocean associated with IOD events. Based on satellite observation data, Delman et al. (2016) also indicated the importance of remote forcing through propagation of equatorial Kelvin waves, and pointed out that anomalous SST cooling south of Java around May–July can be a precursor to the positive IOD. Thus, coastal upwelling along Sumatra and Java is considered to be an essential element of the ocean–atmosphere coupling system in the eastern Indian Ocean.

A detailed vertical structure and its time evolution of the coastal upwelling along the Java coast, however, has not been presented by existing observational studies. Sprintall et al. (2000) reported ocean currents and temperature south of Java based on a mooring, but analyzed the data for a short period during April–June 1997. Syamsudin and Kaneko (2013) analyzed conductivity-temperature-depth (CTD) observation data and along-track shipboard acoustic Doppler current profiler (ADCP) data south of Java, but mainly focused on the current variability along the southern coast of Java. Thus, the actual amplitude, spatial scale, and temporal evolution of the coastal upwelling are not well understood.

Based on the Advanced automatic quality control (AQC) Argo Data prepared by the Japan Agency for Marine-Earth Science and Technology (JAMSTEC), we found that an Argo float drifted in the southeastern tropical Indian Ocean from November 2006 and finally reached the Java coast around mid-July 2008. The Argo float continuously and successfully observed temperature and salinity variations associated with the coastal upwelling every 10 days with fine vertical resolution. In this paper, we document the temperature and salinity variations associated with the coastal upwelling along the southern coast of Java during 2008, a year of the positive IOD event.

2 Data

We used temperature and salinity profiles obtained from AQC Argo Data by JAMSTEC (http://www.jamstec.go.jp/ARGO/argo_web/argo/?lang=en). We focused on an Argo float (WMO number: 5901172), which drifted in the southeastern tropical Indian Ocean from 11 November 2006 to 21 September 2008. To estimate its distance from the Java coast, we used the bathymetry from the ETOPO5 global elevation database on a 1/12° × 1/12° grid (National Oceanic and Atmospheric Administration 1988). In mid-July, the Argo float approached the southern coast of Java (< 90 km) and continued the observation every 10 days. Finally, the float reported the ocean profile on 21 September 2008 at the location 7.59S, 107.19E, less than 20 km from the coast (Fig. 1b), and then lost data communication. According to the quality-check flag of the AQC Argo dataset, no error was reported for the temperature and salinity observation for 0–300 dbar in 2008.

We interpolated the temperature and salinity profiles vertically to every 1 m by the Akima spline method (Akima 1970). Then we estimated the mixed layer depth (MLD) by a density criterion equivalent to an ocean temperature change of 0.5 °C from the surface (Sprintall and Tomczak 1992). Because the topmost observation depth of the Argo float was 5 m or 6 m during 2008, we used the values at 6 m as the surface. We also defined isothermal layer depth (ILD) based on temperature difference from the surface ($\Delta T = 0.5$ °C). The layer between the MLD and the ILD was defined as a barrier layer (Sprintall and Tomczak 1992). We compared the MLD with that on the basis of a shallower depth of the isothermal layer or isopycnal layer (Hosoda et al. 2010), and obtained almost the same result.

To observe the coastal upwelling signals, we also used hourly sea level data from a tidal station at Cilacap (8.25°S, 108.75°E) along the southern coast of Java (Fig. 1). The quality-checked data is available at the website of the University of Hawaii Sea Level Center (UHSLC; Caldwell et al. 2015; available from http://uhslc.soest.hawaii.edu). We prepared a daily sea level anomaly (SLA) time series from the original data with the following procedure. First, barometric effects were corrected by subtracting the sea level pressure data obtained from the European Centre for Medium-Range Weather Forecasts (ECMWF) ERA-Interim reanalysis (Dee et al. 2011). Second, a time series of SLA was calculated from the temporal mean of the time series. Third, we applied a 48-h tide killer filter (Hanawa and Mitsudera 1985) to remove the high-frequency variability associated with semidiurnal and diurnal tides. Finally, we averaged the hourly data to daily data. For more information on the data processing, see Horii et al. (2016).

We used other data sources to study local and large-scale oceanic and atmospheric variations related to the coastal upwelling. SST data was obtained from the National Oceanic and Atmospheric Administration (NOAA) daily optimum interpolation (OI) SST dataset on a 0.25° × 0.25° grid (Reynolds et al. 2007). Using the SST, we defined dipole mode index (DMI) as the difference in SST anomalies between western region (50°E–70°E, 10°S–10°N) and eastern region (90°E–110°E, 10°S–0°). A daily sea surface wind dataset on a 0.25° × 0.25° grid was obtained from the product of the QuikSCAT satellite by Remote Sensing Systems (http://www.remss.com/). A wind stress dataset on a 1° × 1° grid was obtained from the Japanese ocean flux data sets with use of remote sensing observations (J-OFURO; Kubota et al. 2002). To check the reliability of the J-OFURO dataset, we also computed wind stress data with finer spatial resolution (0.25° × 0.25° grid) using the QuikSCAT satellite wind data and standard bulk formula (Large and Pond 1981). To check the relationship between intraseasonal coastal upwelling events and atmospheric intraseasonal variation, we used a well-known Madden–Julian oscillation (MJO; Madden and Julian 1994) index of the real-time multivariate MJO index (Wheeler and Hendon 2004). Satellite-observed SLA was obtained from the SSALTO/DUACS multi-mission altimeter products from Archiving, Validation and Interpretation of Satellite Oceanographic data (AVISO; http://www.aviso.altimetry.fr). We used their gridded products (mapped SLA: MSLA). To estimate the mean seasonal cycle of SLA at the tidal station, we also used along-track SLA data measured by the TOPEX/POSEIDON, JASON-1, and JASON-2 satellites. The anomalies are relative to climatologies based on the data from 1982 to 2011 for the SST, from 2000 to 2008 for the wind and wind stress, and from 1993 to 2012 for the SLA. To focus on time scales longer than 1 week, all data except for Argo data were smoothed with a 7-day running mean filter.

3 Observed coastal upwelling

3.1 Observation south of Java

During 2008, SST anomalies in the tropical Indian Ocean developed to a typical pattern of positive IOD in early May, had the mature phase in August (Fig. 1c), and terminated in September (e.g. Du et al. 2013; Horii et al. 2013). The development, peak, and termination of the 2008 IOD were 2–3 months earlier than the canonical IOD as in 1994, 1997, and 2006 positive IOD events. Due to the advanced seasonal evolution, Du et al. (2013) categorized the 2008 IOD event as an "unseasonable" IOD. Nevertheless, the peak-to-mature phase of the 2008 IOD in May–August corresponded to the season of coastal upwelling south of Java.

Satellite-based SST south of Java exhibited an anomalously cool condition from late May to early September 2008 (Fig. 2a). From January to April 2008, the SST was around 28–29 °C, almost the same as the climatology. Then, the SST significantly decreased in May with an amplitude more than 3 °C in 1 month. It is demonstrated that the SST anomalies south of Java developed about 1 month later than the basin-scale anomalous zonal SST gradient associated with the IOD, as seen in the DMI (Fig. 2b). With some intraseasonal negative peaks in June, late July and late August, the SST anomalies continued to decrease. The anomalous condition ceased in mid-September.

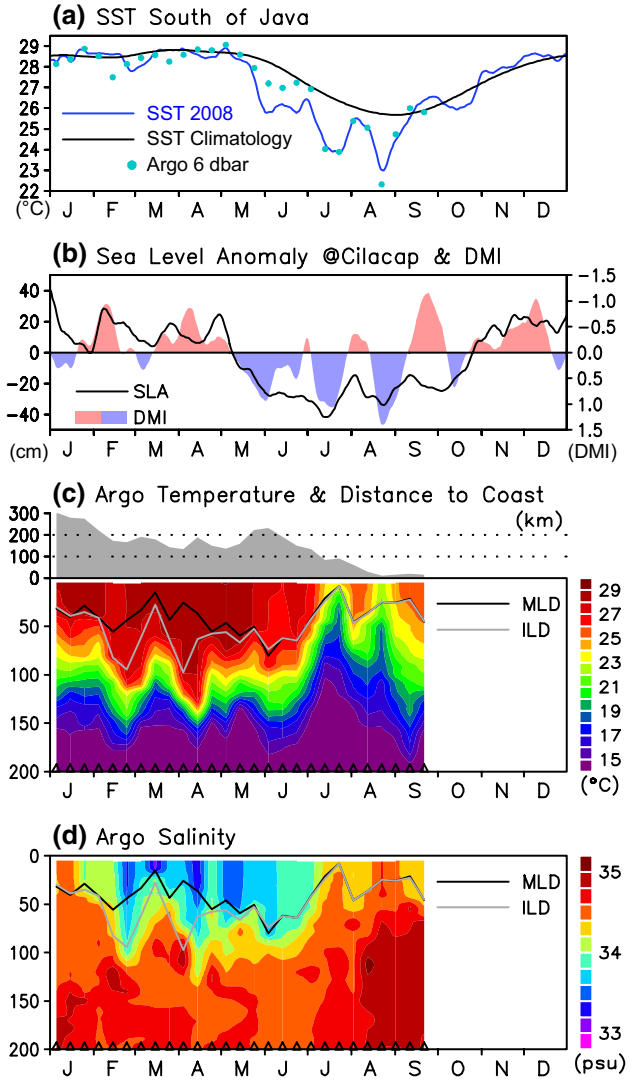

Fig. 2 **a** Time series of SST averaged for the region 106°E–112°E, 9°S–7°S (see Fig. 1b) during 2008 (blue) and the climatology (black). Light-blue dots are temperature at 6 dbar observed by the Argo float around the south of Java. **b** Sea level anomalies (SLA) obtained from the tidal station at the southern coast of Java (black line; left axis). Red/blue shadings show DMI (right axis). Note that the blue shading shows positive DMI (positive IOD). **c** The distance between the Argo float and Java coast (gray shade) and time-depth section of temperature observed by the Argo float (color shade). Small triangles indicate observation points. The black (gray) line shows mixed layer depth (isothermal layer depth). **d** As in Fig. 2c, but for salinity. SST and sea level data are smoothed with a 7-day running mean filter

During May–September, SLA from a tidal station at the southern coast of Java showed almost in-phase variation with the local SST (Fig. 2b). From January to early May, there were intraseasonal variations in SLA (Fig. 2b). An SLA lowering from 25 to −25 cm was observed in May at almost the same time as the local SST. Negative peaks of the SLA variation around mid-July and late August were also concurrent with the SST. The signals of SST cooling, SLA decrease, and southeasterly alongshore winds (Fig. 3) jointly indicate that coastal upwelling occurred along the southern coast of Java, with a larger amplitude than mean seasonal upwelling.

From 5 January to 3 July, an Argo float was drifting off the coastal area of south Java about 130–300 km away from the coast, and measured temperature and salinity (Fig. 2c, d). The temperature in the surface layer (6 dbar) was almost the same as the satellite-based SST, except for June (Fig. 2a). In February and April, a relatively thick barrier layer was observed with intraseasonal deepening events of the thermocline and low-salinity signals at the upper layer (5–50 dbar). During the first half of 2008, the float was probably too far from the coast to capture coastal upwelling signals.

Vertical structures of temperature and salinity associated with coastal upwelling were observed in July–August (Fig. 2c, d). From June to August, the Argo float gradually approached Java and continued the observations. Data was obtained at about 15–90 km from the coast from 13 July to 21 September (Fig. 2c). It was the period when two intraseasonal temperature cooling signals were obtained. In July, the 20 °C (22 °C) isotherm shoaled more than 95 m (90 m). After a month, further cool water upwelled in August. Although there was no surface (0 dbar) observation available in Argo observations, it is likely from the SST and Argo data that the 23-°C isotherm outcropped to the surface. The surface temperature measured by the Argo float and averaged SST were in phase during the two intraseasonal events (Fig. 2a). Concurrent with these upward displacements of cold thermocline water, high-salinity signals extended upward in July and August, respectively (Fig. 2d). Due to the stratification by vertical temperature gradient, there was no barrier layer from June to September.

During the period 13 July to 21 September, the SST observed by the Argo float (6 dbar) agreed well with the satellite-based SST south of Java (Fig. 2a). The amplitudes of SST observed by the Argo float and that by satellite were comparable (1.2 and 1.0 °C, respectively), the mean difference was less than 0.1 °C, and the root mean square (RMS) difference was 0.4 °C.

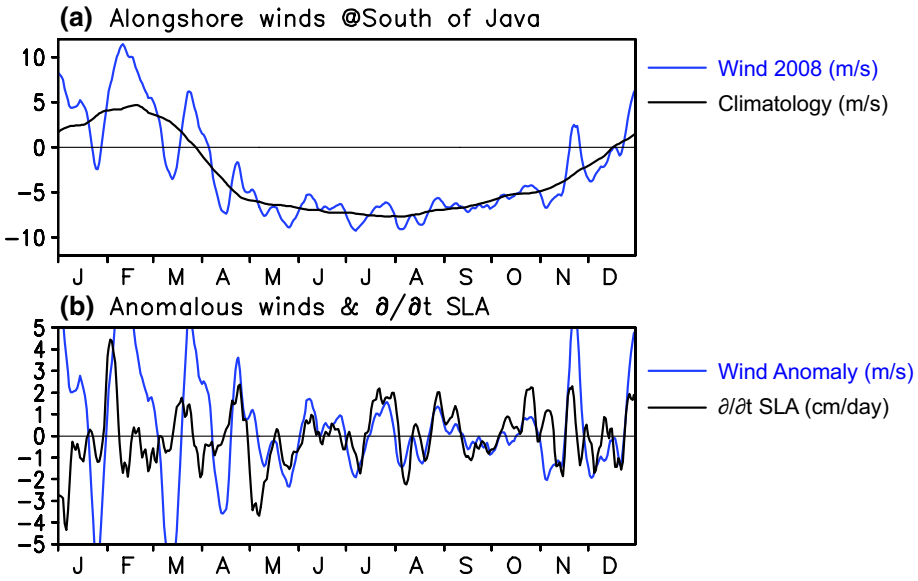

Fig. 3 **a** Time series of alongshore wind averaged for the region 106°E–112°E, 9°S–7°S (Fig. 1b) during 2008 (blue) and the climatology (black). Positive values denote southeastward alongshore wind. The averaged region is shown in Fig. 1b. **b** Wind anomaly (blue) and temporal change of the SLA at the southern coast of Java (black) observed by a tidal station at Cilacap. Data are smoothed with a 7-day running mean filter

3.2 Local wind forcing

Climatological local wind south of Java was dominated by southeasterly (northwesterly) alongshore winds in the boreal summer (winter; Fig. 3a). In general, seasonal variation of alongshore winds in 2008 was similar to the climatology. The wind from January to April in 2008 fluctuated on an intraseasonal time scale, reflecting the strong influence of the MJO in the equatorial Indian Ocean (Matthews et al. 2010). The direction of dominant winds turned from northwesterly to southeasterly in April as the climatology, and the southeasterly phase continued to December.

Because observed SLA along the coast has finer temporal resolution than Argo data, we compared the SLA variation to the local alongshore winds to explore local atmospheric forcing and ocean response (Fig. 3b). During the southeasterly phase (May–October), anomalous alongshore winds (m/s) and time change of SLA (cm/day) at the southern coast of Java were in phase with a significant correlation of 0.56. Here, the mean seasonal SLA cycle was removed using the along-track SLA data from AVISO (See Horii et al. 2016 for the detailed procedure). Assuming that ocean response to wind stress forcing can be simplified with a linear two-layer model, upwelling velocity (w) is proportional to the wind stress (τ; Yoshida 1955). Given the one-dimensional oceanic vertical process, time change of thermocline and sea level ($\partial h/\partial t$) are in phase with the wind forcing, as observed from May to October (Fig. 3b).

To check the relationship between the intraseasonal coastal upwelling events and atmospheric intraseasonal variation, we investigated MJO indices, intraseasonal winds, and the periods of upwelling events. Southeasterly wind forcing along the coasts of Sumatra and Java were associated with atmospheric intraseasonal variation (Fig. 4). The intraseasonal alongshore winds and time change of the sea level ($\partial h/\partial t$) are correlated with a significant correlation of 0.55 (significant at 90% level). The index of real-time multivariate MJO series 2, the negative peak of which shows MJO-related convective peak in the eastern Indian Ocean (Wheeler and Hendon 2004), are also significantly correlated with the intraseasonal alongshore winds (correlation coefficient: 0.78) with a 9-day lag. Here, the alongshore winds lead the MJO index. The result suggests alongshore winds are associated with the easterly phase of the MJO.

The relationship between the winds and the sea level was completely different during January–April and November–December (Fig. 3b). These results indicate that the two-layer approximation of the coastal upwelling system is only valid during May–October with background southeasterly winds. During November–April, MJO-related intraseasonal forcing in the equatorial Indian Ocean may influence the sea level variation through propagation of Kelvin waves and cause the discrepancies (Chen et al. 2016; Delman et al. 2016). In the next section, we will focus on the local wind forcing and quantify the ocean response.

3.3 Large-scale atmosphere and ocean variation

We observe large-scale atmospheric and oceanic signals associated with the coastal upwelling events. Figure 5 shows zonal/alongshore winds, satellite-observed SLA, and SST in the entire equatorial Indian Ocean and along the coasts of Sumatra and Java. In January to April, there were several westerly wind events in the zonal wind anomalies. These westerly wind events excited some eastward-propagating anomalously positive SLA signals observed in January–April (Delman et al. 2016). During the period, there

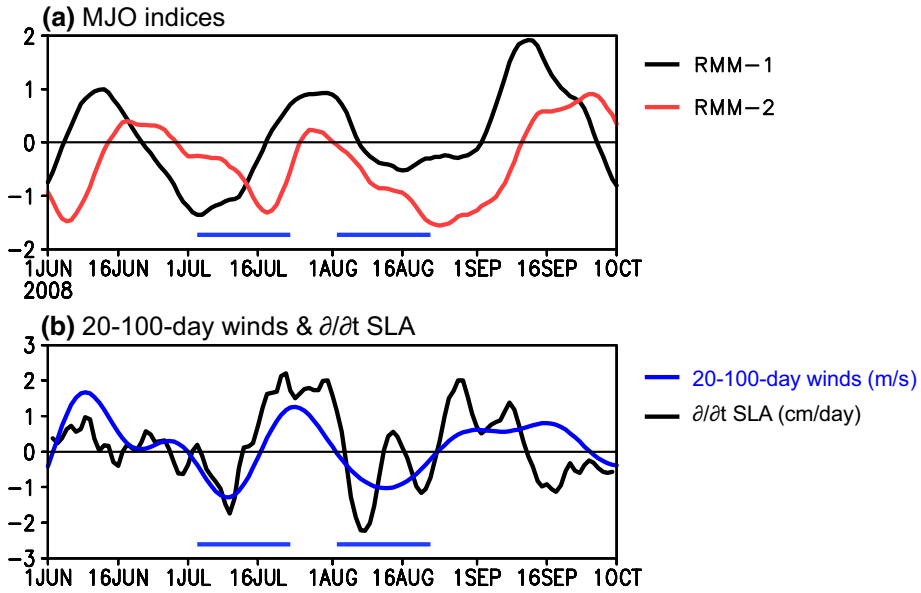

Fig. 4 **a** MJO indices by Wheeler and Hendon (2004) during June–September 2008. The black (red) line shows the real-time multivariate MJO (RMM) series-1 (series-2). **b** Time series of alongshore wind (20-100-day filtered) along the coasts of Sumatra, Java, and Bali (98°E–120°E; blue) and SLA at the southern coast of Java (black) observed by a tidal station at Cilacap during June–September 2008. Horizontal blue lines show the periods of coastal upwelling events observed by the Argo float

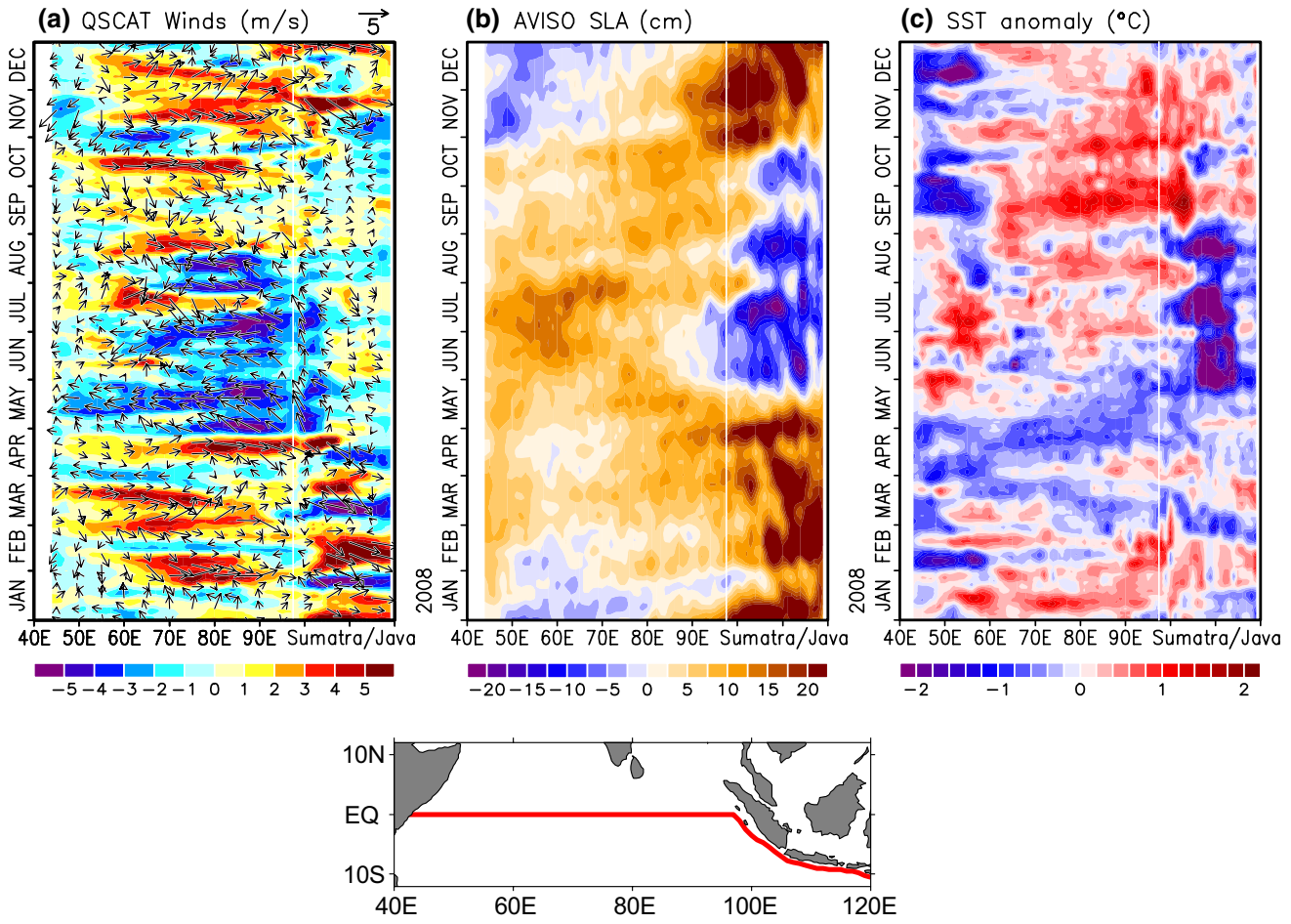

Fig. 5 Longitude-time sections of **a** wind anomalies, **b** SLA, and **c** SST anomalies along the equator (40°E–97°E) and the coasts of Sumatra, Java, and Bali (98°E–120°E) during 2008. Color shades in **a** show the zonal and alongshore winds. The bottom panel shows the section with the red line. Data are smoothed with a 7-day running mean filter

was no significant anomalous SST development except for the intraseasonal signals.

In May, basin-wide equatorial easterly wind anomalies occurred with southeasterly wind anomalies along the coasts of Sumatra and Java (Fig. 5). SLA turned to negative with development of cool SST anomalies along the coasts. Such large-scale easterly and southeasterly wind anomalies along the equator and the coasts of Sumatra and Java continued to late August with some intraseasonal negative peaks (Figs. 4b, 5a). The SST anomalies show three intraseasonal-scale negative peaks in June, July, and August as in Fig. 2a. Warm SST anomalies also occurred during June–August in the equatorial Indian Ocean and formed anomalous SST gradients. The SST difference from the equatorial eastern Indian Ocean (29.5 °C) to south of Java (< 24 °C) exceeded 5 °C. After the termination of the IOD in September, there was a minor negative peak of SLA along the coast in October with southeasterly wind anomalies in mid-September to mid-October. The signal in SST anomalies was rather small compared with that during June–August. These features observed during this particular period in 2008 are consistent with Delman et al. (2016). They estimated the amplitude of equatorial Kelvin waves by satellite data and indicated that the SST anomalies south of Java can be explained by the remote wind forcing and eastward propagation of upwelling Kelvin waves.

The Argo float observed vertical structures in July–September near the Java coast (Fig. 2c, d) when the SST anomalies exhibited the second and third significant negative peaks (Fig. 5). The first peak of the cool SST anomalies in June was not captured by the float, probably because the float was too distant from the coast. Almost all significant negative SST anomalies were observed along the southern coast of Java (105°E–115°E), but were less along Sumatra. From these results, the ocean variations observed by the Argo float during July–September can be interpreted as an evolution of intraseasonal-scale coastal upwelling events on the altered background condition, i.e. elevated thermocline due to the positive IOD events.

4 Discussion

The Argo float data in 2008 provide an excellent opportunity to study the coastal upwelling along the southern coast of Java. In this section, we quantify the local wind forcing and observed coastal upwelling signals. We also discuss implications of the observed signal and development of the positive IOD event.

We estimated upwelling velocity from the local wind forcing and compared it to upward thermocline movements observed by the Argo float during 3–23 July and 2–22 August. Assuming a two-layer model (Yoshida 1955), the coastal upwelling velocity w can be estimated as $w = \tau/\rho\ (g' H)^{1/2}$, where τ is alongshore southeasterly wind stress for the Java coast, ρ is the density of the upper layer, $g' = g\ \Delta\rho/\rho$ is the reduced gravity, g is the gravity, $\Delta\rho$ is the density difference between the upper and lower layers, and H is the thickness of the upper layer. We estimated ρ, $\Delta\rho$, and τ based on the observed temperature and salinity and anomalous alongshore wind stress from June–August. From observed vertical temperature structures, we assumed $H = 10$, 30, and 50 m as the upper layer thickness. The density (ρ) and density difference ($\Delta\rho$) were estimated accordingly for the assumed H, with vertical density profiles obtained from the Argo float. We used the density value from surface (6 dbar) to bottom (679 dbar) for the calculation, with reference to the average depth of the continental shelf within 50 km off the southern coast of Java. The average amplitudes of the anomalous wind stress during 3–23 July and 2–22 August were 0.007 N/m^2 and 0.017 N/m^2, respectively. The amplitude of wind stress in the coastal area was almost the same using the wind stress calculated by the QuikSCAT winds and standard bulk formula.

Figure 6 summarizes the results. During 3–23 July (Fig. 6a), upwelling velocity was estimated to be 0.41–0.88 (m/day) and underestimates the upward movement of the observed 20- and 22-°C isotherms (3.55 m/day and 2.98 m/day, respectively). On the other hand, the estimated upwelling velocity during 2–22 August (0.99–2.12 m/day) roughly agreed well with the observed thermocline variation (1.64 and 2.53 m/day; Fig. 6b). It should be noted that the Argo float observed the ocean temperature in July drifting toward the coast (Fig. 2c). It probably observed spatially different ocean vertical structures of a deep thermocline at the offshore region and shallow thermocline at the coastal region, and overestimated the local temperature change. Another reason to cause the difference in July would be an influence from remote forcing through the propagation of Kelvin waves (Fig. 5b), as shown in Delman et al. (2016). There was an easterly wind event in the central-eastern equatorial Indian Ocean from mid-June to mid-July with eastward propagation of negative SLA, and that was larger than the subsequent easterly wind event from late July to mid-August (Fig. 5a, b).

The spatial scale of coastal upwelling can be estimated as the first internal Rossby radius $(g' H)^{1/2}/f$, where f is the Coriolis parameter (Yoshida 1955). The small f at this low latitude (8°S) yields a horizontal scale of 33 km, 57 km, and 72 km of the coastal upwelling, for $H = 10$, 30, and 50 m, respectively. These results indicate that the Argo float successfully observed an intraseasonal-scale coastal upwelling event along the southern coast of Java in August 2008.

It is of interest to know how the observed coastal upwelling is related to the occurrence of the positive IOD in 2008. Delman et al. (2016) pointed out that anomalous

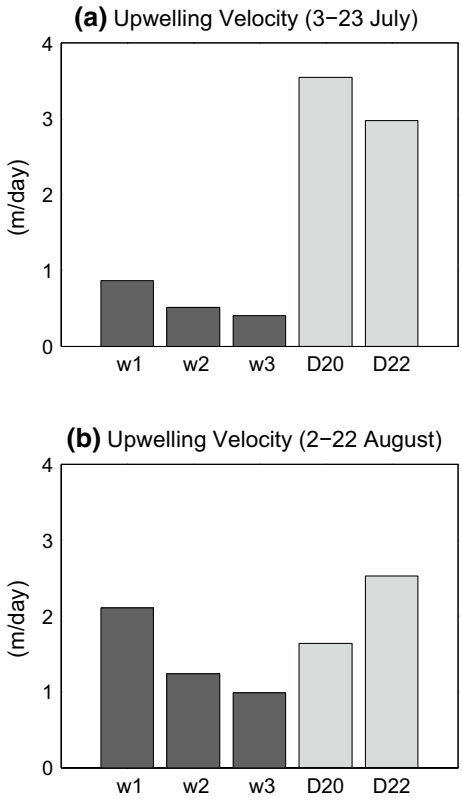

Fig. 6 Coastal upwelling velocities estimated by the anomalous alongshore wind stress (w1–w3) and upward movements of the 20- and 22-°C isotherm observed by the Argo float (D20 and D22). The periods are **a** 3–23 July and **b** 2–22 August. The upwelling velocities w1, w2, and w3 were estimated assuming the upper layer thickness as $H = 10$, 30, and 50 m, respectively

SST cooling south of Java can be a precursor to a positive IOD. In the case of 2008, a large-scale anomalous zonal SST gradient initiated in early May (DMI in Fig. 2b) before the observation of the coastal upwelling during July–August. Therefore, the observed coastal upwelling events must not be the cause of the positive IOD events. Significant cooling of local SST and ocean temperature during July–August likely resulted from intraseasonal-scale anomalous southeasterly alongshore winds (Fig. 4b) on the background of a shallow thermocline during the peak phase of the 2008 positive IOD. Nevertheless, the intraseasonal-scale coastal upwelling possibly contributed to the development of the IOD, providing anomalously cold thermocline water to the mixed layer. During the IOD, the temperature anomalies upwell in the coastal area, then are advected westward by anomalous westward surface currents, and lead to the anomalous SST cooling in the broad eastern Indian Ocean (Horii et al. 2009). It is demonstrated from the vertical temperature structures (Fig. 2) that the intraseasonal-scale coastal upwelling strengthened the entrainment of cold water to the surface layer. Thus, the coastal upwelling must be an important source of cold anomalies for the IOD development.

Finally, a question is if an enhanced regional-scale SST gradient at the southeastern edge of the warm pool (Fig. 1a) and resultant atmospheric response further enhances the SST gradient. The horizontal scale of the coastal upwelling is rather small (less than 100 km) compared with that of a climate mode. Regional-scale air-sea interaction along the coasts of Sumatra and Java may possibly be embedded in the basin-scale climate mode, i.e. positive IOD. We will focus on heat balance analyses for coastal regions around the coasts of Sumatra and Java and diagnose the air-sea feedback (Jin et al. 2006) in future studies.

5 Summary and conclusion

In the present study, we have documented the amplitude and evolution of the coastal upwelling along the southern coast of Java, using data from an Argo float. During the peak of the positive IOD event in 2008, the Argo float successfully observed vertical structures of temperature and salinity associated with the coastal upwelling in the coastal area. Two intraseasonal-scale coastal upwelling events were observed in July and August with significant upward thermocline movement, anomalous southeasterly alongshore winds, and lowering of local SLA and SST. Based on a two-layer model approximation, we quantified the coastal upwelling signal with local atmospheric forcing. In August, when the float was located within 90 km from Java, the estimated upwelling velocity by the anomalous wind stress agreed well with the observed temperature variations.

Although this report provides vertical structures on how ocean temperature and salinity fluctuate with the coastal upwelling, the observations are taken only at the limited locations and time for less than a year. Future observations around the coasts of Sumatra and Java are needed to clarify the general feature of the upwelling system. Under the CLIVAR Indian Ocean Panel of the World Climate Research Program, the Eastern Indian Ocean Upwelling Research Initiative (EIOURI) is proposed to understand the processes of the coastal upwelling and their impacts on the local biogeochemical balance and ecosystems (Yu et al. 2016). Further studies based on the international collaborative observations are necessary for better understanding of the coastal upwelling and its possible impact on climate.

Acknowledgements AQC Argo data version 1.2 produced by JAMSTEC is used for this study (available online at http://www.jamstec.go.jp/ARGO/argo_web/argo/?page_id=100&lang=en). We thank UHSLC (http://uhslc.soest.hawaii.edu) for providing quality-controlled sea level data from tide gauges. We also thank the following data providers: NOAA OISST data were provided by NOAA/OAR/ESRL PSD, Boulder, Colorado, USA, from their website (http://www.esrl.noaa.gov/

psd/); Wind data of the QuikSCAT satellite were provided by Remote Sensing Systems (available online at http://www.remss.com); The altimeter products were produced by Ssalto/Duacs and distributed by AVISO, with support from Cnes; and wind stress data in the J-OFURO data set were provided by Tokai University (http://dtsv.scc.u-tokai.ac.jp/j-ofuro/index.html). We thank Y. Masumoto, M. Nagura and K. J. Richards for helpful discussions. This study was financially supported by the Ministry of Education, Culture, Sports, Science and Technology, Japan, Grants-in-Aid for Scientific Research for Young Scientists (B), 25800270.

References

Akima H (1970) A new method of interpolation and smooth curve fitting based on local procedures. J Assoc Comput Mach 17:589–602

Bray NA, Hautala S, Chong JC, Pariwono J (1996) Large-scale sea level, thermocline, and wind variations in the Indonesian throughflow region. J Geophys Res 101:12239–12254

Caldwell PC, Merrifield MA, Thompson PR (2015) Sea level measured by tide gauges from global oceans—the Joint Archive for Sea Level holdings (NCEI Accession 0019568) Version 5.5. NOAA National Centers for Environmental Information, Dataset, https://doi.org/10.7289/v5v40s7w

Chen GD, Han WQ, Li YL, Wang DX, Shinoda T (2015) Intraseasonal variability of upwelling in the equatorial eastern Indian Ocean. J Geophys Res Oceans 120:7598–7615. https://doi.org/10.1002/2015JC011223

Chen GD, Han WQ, Li YL, Wang DX (2016) Interannual variability of equatorial eastern Indian Ocean upwelling: local versus remote forcing. J Phys Oceanogr 46:789–807. https://doi.org/10.1175/JPO-D-15-0117.1

Dee DP, Uppala S, Simmons A, Berrisford P, Poli P, Kobayashi S, Andrae U, Balmaseda M, Balsamo G, Bauer P et al (2011) The ERA-interim reanalysis: configuration and performance of the data assimilation system. Q J R Meteorol Soc 137(656):553–597

Delman AS, Sprintall J, McClean JL, Talley LD (2016) Anomalous Java cooling at the initiation of positive Indian Ocean Dipole events. J Geophys Res Oceans 121:5805–5824. https://doi.org/10.1002/2016JC011635

Du Y, Qu T, Meyers G, Masumoto Y, Sasaki H (2005) Seasonal heat budget in the mixed layer of the southeastern tropical Indian Ocean in a high-resolution general circulation model. J Geophys Res 110:C04012. https://doi.org/10.1029/2004JC002845

Du Y, Cai W, Wu Y (2013) A new type of the Indian Ocean Dipole since the mid-1970s. J Clim 28:959–972

Farley JH, Davis TL (1998) Reproductive dynamics of southern bluefin tuna, *Thunnus maccoyii*. Fish Bull 96:223–236

Halkides DJ, Lee T (2009) Mechanisms controlling seasonal-to-interannual mixed layer temperature variability in the southeastern tropical Indian Ocean. J Geophys Res 114:C02012. https://doi.org/10.1029/2008JC004949

Hanawa K, Mitsudera H (1985) On the data processing of daily mean values of oceanographic data: note on the daily mean sea-level data (in Japanese). Bull Coastal Oceanogr 23:79–87

Horii T, Masumoto Y, Ueki I, Hase H, Mizuno K (2009) Mixed layer temperature balance in the eastern Indian Ocean during the 2006 Indian Ocean dipole. J Geophys Res 114:C07011. https://doi.org/10.1029/2008JC005180

Horii T, Ueki I, Ando K (2013) Contrasting development and decay processes of Indian Ocean Dipoles in the 2000s. SOLA 9:183–186. https://doi.org/10.2151/sola.2013-041

Horii T, Ueki I, Syamsudin F, Sofian I, Ando K (2016) Intraseasonal coastal upwelling signal along the southern coast of Java observed using Indonesian tidal station data. J Geophys Res Oceans 121:2690–2708. https://doi.org/10.1002/2015JC010886

Hosoda S, Ohira T, Sato K, Suga T (2010) Improved description of global mixed-layer depth using Argo profiling floats. J Oceanogr 66:773–787

Iizuka S, Matsuura T, Yamagata T (2000) The Indian Ocean SST dipole simulated in a coupled general circulation model. Geophys Res Lett 27:3369–3372

Iskandar I, Rao S, Tozuka T (2009) Chlorophyll–a bloom along the southern coasts of Java and Sumatra during 2006. Int J Remote Sens 30:663–671

Jin FF, Kim ST, Bejarano L (2006) A coupled-stability index for ENSO. Geophys Res Lett 33:L23708. https://doi.org/10.1029/2006GL027221

Kubota M, Iwasaka N, Kizu S, Konda M, Kutsuwada K (2002) Japanese ocean flux data sets with use of remote sensing observations (JOFURO). J Oceanogr 58:213–225

Large WG, Pond S (1981) Open ocean momentum flux measurements in moderate to strong winds. J Phys Oceanogr 11:324–336

Madden RA, Julian PR (1994) Observations of the 40–50-day tropical oscillation—A review. Mon Weather Rev 122:814–837

Matthews A, Singhruck P, Heywood K (2010) Ocean temperature and salinity components of the Madden-Julian oscillation observed by Argo floats. Clim Dyn 35(7–8):1149–1168. https://doi.org/10.1007/s00382-009-0631-7

Murtugudde R, McCreary JP, Busalacchi AJ (2000) Oceanic processes associated with anomalous events in the Indian Ocean with relevance to 1997–1998. J Geophys Res 105:3295–3306

National Oceanic and Atmospheric Administration (1988) Digital relief of the surface of the earth, data announcement 88-MGG-02. Natl Geophys Data Cent, Boulder

Ningsih NS, Rakhmaputeri N, Harto AB (2013) Upwelling variability along the southern coast of Bali and in Nusa Tenggara waters. Ocean Sci J 48:49–57

Reynolds RW, Smith TM, Liu C, Chelton DB, Casey KS, Schlax MG (2007) Daily high-resolution-blended analyses for sea surface temperature. J Clim 20:5473–5496

Saji NH, Goswami BH, Vinayachandran PN, Yamagata T (1999) A dipole mode in the tropical Indian Ocean. Nature 401:360–363

Schott FA, Xie S-P, McCreary JP Jr (2009) Indian Ocean circulation and climate variability. Rev Geophys 47:1002. https://doi.org/10.1029/2007rg000245

Sprintall J, Tomczak M (1992) Evidence of the barrier layer in the surface layer of the tropics. J Geophys Res 97:7305–7316

Sprintall J, Gordon AL, Murtugudde R, Susanto RD (2000) A semiannual Indian Ocean forced Kelvin wave observed in the Indonesian seas in May 1997. J Geophys Res 105:17217–17230

Susanto RD, Marra J (2005) Effects of the 1997/98 El Nino on Chlorophyll a variability along the southern coasts of Java and Sumatra. Oceanography 18:124–127. https://doi.org/10.5670/oceanog.2005.13

Susanto RD, Gordon AL, Zheng QN (2001) Upwelling along the coasts of Java and Sumatra and its relation to ENSO. Geophys Res Lett 28:1599–1602

Syamsudin F, Kaneko A (2013) Ocean variability along the southern coast of Java and Lesser Sunda Islands. J Oceanogr 69:557–570

Vinayachandran PN, Iizuka S, Yamagata T (2002) Indian Ocean dipole mode events in an ocean general circulation model. Deep-Sea Res Part (II) 49:1573–1596

Webster PJ, Moore AM, Loschnigg JP, Leben RR (1999) Coupled ocean–atmosphere dynamics in the Indian Ocean during 1997–98. Nature 401:356–360

Wheeler M, Hendon H (2004) An all-season real-time multivariate MJO index: development of an index for monitoring and prediction. Mon Weather Rev 132:1917–1932

Wyrtki K (1962) The upwelling in the region between Java and Australia during the south east monsoon. Aust J Mar Freshw Res 17:217–225

Yoshida K (1955) Coastal upwelling off the California coast. Rec Oceanogr Works, Japan 15:1–13

Yu W, Hood R, D'Adamo N, McPhaden MJ et al (2016) The EIOURI Science Plan. ESSO—Indian National Centre for Ocean Information Services (INCOIS). Hyderabad India. http://www.iioe-2.incois.gov.in/IIOE-2)